Comparing the Biogeochemistry of Storm Surge Sediments and Pre-storm Soils in Coastal Wetlands: Hurricane Irma and the Florida Everglades

Joshua L. Breithaupt[1] · Nia Hurst[1] · Havalend E. Steinmuller[1] · Evan Duga[1] · Joseph M. Smoak[2] · John S. Kominoski[3] · Lisa G. Chambers[1]

Abstract

Hurricanes can alter the rates and trajectories of biogeochemical cycling in coastal wetlands. Defoliation and vegetation death can lead to increased soil temperatures, and storm surge can variously cause erosion or deposition of sediment leading to changes in soil bulk density, nutrient composition, and redox characteristics. The objective of this study was to compare the biogeochemistry of pre-storm soils and a carbonate-rich sediment layer deposited by Hurricane Irma that made landfall in southwest Florida as a category 3 storm in September 2017. We predicted that indicators of biogeochemical activity (e.g., potential soil respiration rates, microbial biomass (MBC), and extracellular enzyme activities) would be lower in the storm sediment layer because of its lower organic matter content relative to pre-storm soils. There were few differences between the storm sediment and pre-storm soils at two of the sites closest to the Gulf of Mexico (GOM). This suggests that marine deposition regularly influences soil formation at these sites and is not something that occurs only during hurricanes. At a third site, 8 km from the GOM, the pre-storm soils had much greater concentrations of organic matter, total N, total P, MBC, and higher potential respiration rates than the storm layer. At this same site, CO_2 fluxes from intact soil cores containing a layer of storm sediment were 30% lower than those without it. This suggests that sediment deposition from storm surge has the potential to preserve historically sequestered carbon in coastal soils through reduced respiratory losses.

Keywords Hurricane Irma · Mangroves · Soil respiration · Sediment deposition · Organic carbon · Inorganic carbon · Nutrient biogeochemistry

Introduction

Due to their exposed position at the land-sea interface, mangrove forests are capable of providing coastal protection from tropical storms and hurricanes (Arkema et al. 2013). They often receive the brunt of the wind energy (Doyle et al. 1995) and slow and reduce the depth of storm surge (Krauss

et al. 2009; Zhang et al. 2012). Providing this protection can come at a high cost to the forest structure and function, with the potential for extensive defoliation, uprooting, and mortality of the trees (McCoy et al. 1996; Kauffman and Cole 2010; Salmo et al. 2014; Long et al. 2016). The high frequency of storms is a likely driver of relatively low complexity index values of mangrove forests compared to their inland forest counterparts (Roth 1992). Storm impacts cause ecosystem damage that can last for years (Danielson et al. 2017) or that may be irreversible (Cahoon et al. 2003). However, mangrove ecosystems can also be considerably resilient to such disturbance. Even when initial storm damage is severe, the deleterious effects at the ecosystem scale have often been relatively short in duration. For example, up to 90% recovery was observed within 18 months in severely damaged mangroves of the Philippines following Super Typhoon Haiyan (Long et al. 2016) and full recovery of net primary production within 5 years has been documented for some regions of the

---

Communicated by Marco Bartoli

✉ Joshua L. Breithaupt
  Josh.Breithaupt@gmail.com

[1] University of Central Florida, Orlando, FL 32816, USA

[2] University of South Florida, St. Petersburg, FL 33701, USA

[3] Department of Biological Sciences, Florida International University, Miami, FL 33199, USA

Florida Everglades following Hurricane Wilma (Danielson et al. 2017). When examined over multi-annual timescales, the effect of storms may be beneficial for mangrove wetlands responding to rising sea levels. Storms are capable of increasing sediment accretion (Smoak et al. 2013) and surface elevation (Cahoon 2006; Whelan et al. 2009), as well as providing a subsidy of nutrients capable of stimulating forest productivity (Castañeda-Moya et al. 2010; Salmo et al. 2014).

Mangrove wetlands are globally important regions of carbon cycling and sequestration (Jennerjahn and Ittekkot 2002; Bouillon et al. 2008; Donato et al. 2011; Maher et al. 2018). Large storms can affect carbon stocks and cycling rates both positively and negatively. Carbon losses may occur due to decreased live biomass (Smith et al. 2009; Salmo et al. 2014; Danielson et al. 2017) and potentially severe erosion or collapse of peat soil (Cahoon et al. 2003). Extensive defoliation and tree mortality can increase understory light levels and temperature (Sherman et al. 2001; Barr et al. 2012; Salmo et al. 2014), contributing to enhanced mineralization of soil organic matter. Conversely, instead of the negative effects associated with erosion, storm surge has also been documented to scour sediment from the marine environment and deposit it within coastal wetlands (Smith et al. 2009; Whelan et al. 2009; Castañeda-Moya et al. 2010; Smoak et al. 2013). Benefits stemming from this sediment deposition include elevated rates of organic carbon (OC) burial (Smoak et al. 2013). Storm surge deposition of high-density mineral sediment could also increase OC retention in the underlying soils by creating a burial cap that prevents oxygen penetration into the soil, promoting more anaerobic conditions and decreasing respiration of CO_2 (Croft et al. 2006; Salmo et al. 2014). Because storms have the capacity to substantively alter the physicochemical properties and composition of surface soils, it is important to quantify the magnitude of these changes and their effect on microbially mediated carbon cycling and nutrient availability.

We compared surface and subsurface soil biogeochemistry and microbial activities along a coastal-to-inland gradient following Hurricane Irma (2017), assuming subsurface soils represent pre-hurricane-derived and surface soils represent hurricane-derived soils/sediments. Our objectives were to (1) quantify carbon and nutrient deposition rates, soil microbial community size (microbial biomass), and microbial activity (respiration rates and extracellular enzyme activity), in the storm-derived sediments and underlying pre-storm soils, and (2) examine the potential of the storm sediment layer to enhance regional carbon sequestration by increasing organic carbon burial and reducing atmospheric flux of CO_2 from pre-storm soil. Based on observations from previous large storms, we predicted that Irma deposition rates of OC, TN, and TP would be higher than historical annual averages at these sites. Second, we predicted that indicators of biogeochemical activity (e.g., potential soil respiration rates, microbial biomass, and extracellular enzyme activities) would be lower in the

Irma layer compared to underlying soils because of the unique physiochemical properties of the storm sediments. Thirdly, we predicted lower atmospheric fluxes of CO_2 from soils covered by the storm layer compared to those without the layer because of the high bulk density and low-organic content of storm sediment.

Methods

Study Region

Coastal ecosystems of southwestern Florida are frequently exposed to disturbance from tropical storms and hurricanes (Smith et al. 1994). Most recently, Hurricane Irma made landfall on Cudjoe Key, FL, approximately 85 km southwest of the mouth of the Shark River in Everglades National Park (ENP), on September 11, 2018 with maximum sustained wind speeds of 213 km h^{-1} (Cangialosi et al. 2018). Coastal water levels within ENP due to the combination of tides and storm surge were estimated at 1.8–3.0 m above sea level, and rainfall was between 25.4 and 38.1 cm (Cangialosi et al. 2018).

Field samples were collected from three sites on the Shark River in Everglades National Park. The three sites, SRS-7b, SRS-6, and SRS-5, were 2, 4, and 8 km respectively from the Gulf of Mexico (GOM) (Fig. 1). This sampling design was intended to observe the difference between storm-derived sediments and pre-storm soils at these sites and was not intended as a survey of storm sediment deposition across the region, which was shown to be highly variable, ranging from no deposition up to 9 cm (Radabaugh et al. 2019). Sampling was conducted on January 4, 2018, approximately 4 months after the storm's occurrence. Stations SRS-5 and SRS-6 are part of the Florida Coastal Everglades Long Term Ecological Research program. Station SRS-7b coincides with previously reported soil nutrient content and ^{210}Pb dates referred to as site WSC-6 in Breithaupt et al. (2017, 2019). Salinity of porewater ($\sim$ 5–10 cm depth) was measured at each site using a handheld refractometer. Values were 31, 25, and 10 for sites SRS-7b, 6, and 5, respectively.

Storm Depth Measurements, Core Collection, and Soil Characterization

Soil cores (6.9 cm diameter; depth dimensions provided below) were collected approximately 10 m from the river's edge at each site to capture a substantial storm layer. The depth of sediment deposited by Irma was discernible from the pre-storm soil because of its gray color and clay-rich texture that readily separated from the underlying soil, often with a layer of leaf litter in between (Fig. 2a). Three soil push cores were collected at each site for destructive sampling. The thickness of the storm layer was measured in three positions around the

Fig. 1 Sampling locations on the Shark River in Everglades National Park, FL, USA. Sites SRS-7b, SRS-6, and SRS-5 are 2, 4, and 8 km respectively from the Gulf of Mexico. Note that all subsequent figures are oriented following this spatial pattern, with SRS-7b on the left and SRS-5 to the right
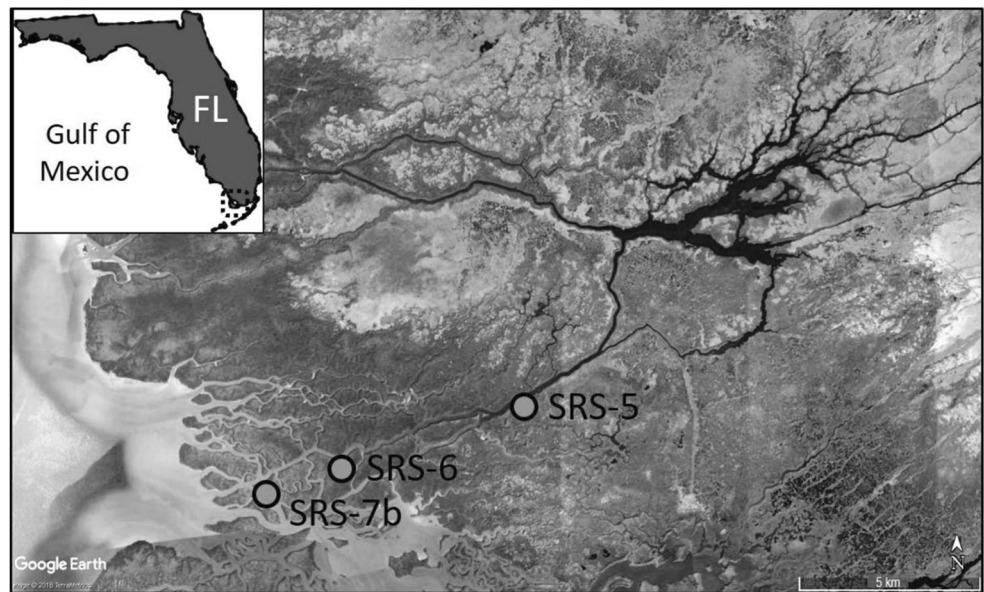

exterior of each core. Cores were subsequently extruded and cut in the field, separating the storm layer (2–3 cm, depending on location) and underlying ~ 5 cm of soil from each core into pre-weighed, airtight bags, and stored on ice until return to the laboratory.

Soils were weighed for total wet weight and then homogenized; aliquots were collected, weighed, and dried at 70 °C until constant weight was achieved. Moisture content was calculated as the percentage of mass lost between wet and dry measurements. Dry bulk density (DBD) was calculated by subtracting soil moisture from the mass of wet soil divided by the volume of the coring tube for the depth of each extruded core segment.

After drying, all soil samples were homogenized using a Spex 8000 mixer/mill (Spex Sample Prep, Metuchen, NJ, USA). Soil organic matter (SOM) content was determined via loss-on-ignition (LOI) at 550 °C for 3 h, followed by a subsequent LOI at 990 °C for 1 h to determine the $CaCO_3$ content (Dean 1974). Measurements of soil total C, OC, inorganic C (IC), and total N (TN) were conducted using an Elementar vario MICRO cube (Elementar Analytical, Langenselbold, Germany). For OC, sediment was de-carbonated by fumigation with 12 N HCl in a desiccator for 6 h (Harris et al. 2001). Inorganic C was calculated as the difference between total C and OC. Total P was measured following Andersen (1976) by digesting

Fig. 2 **a** Photograph of Irma storm layer sediment atop pre-storm soil at site SRS-5, as well as mean (± 1 SE) site values for **b** accretion, **c** mass deposition (including $CaCO_3$, and soil organic matter [SOM]), **d** carbon deposition (including inorganic and organic carbon [IC and OC]), **e** total nitrogen (TN) deposition, and **f** total phosphorus (TP) deposition. Different capital and lowercase letters and numbers within panels indicate significant differences between sites for individual deposition parameters. Statistical results of comparisons are provided in Table 1
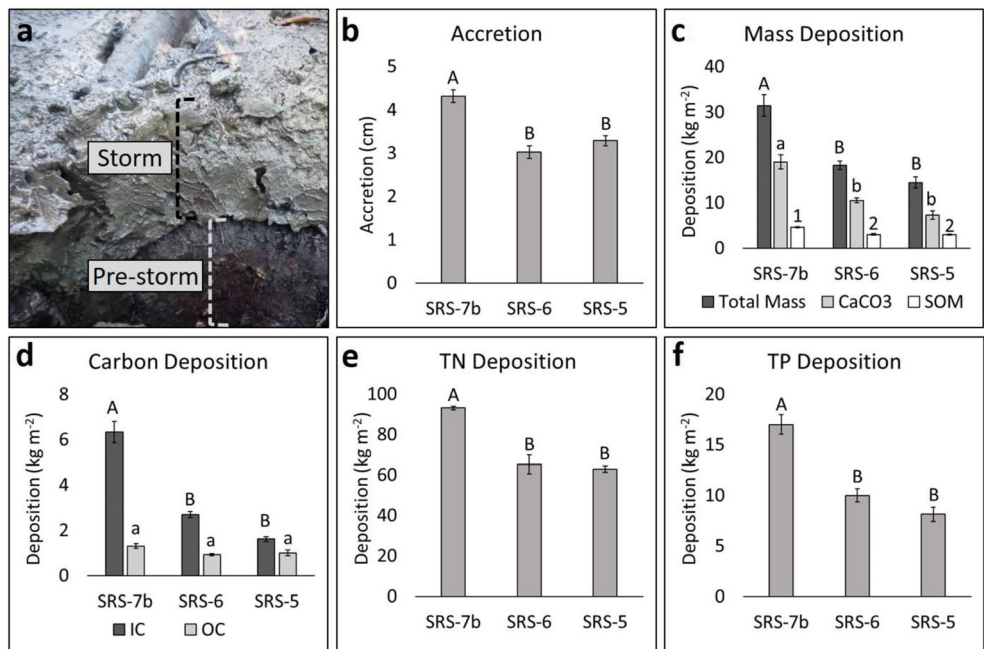
combusted samples in 1 M HCl and colorimetrically analyzing the digestate with a SEAL AQ2 Automated Discrete Analyzer (Seal Analytical, Mequon, WI) using EPA method 365.1 Rev. 2.0 (USEPA 1993).

Total storm deposition of sediment mass, SOM, OC, IC, $CaCO_3$, TN, and TP was calculated by multiplying storm DBD (g cm^{-3}) and accretion depths (cm) by the soil concentrations (%) of each constituent. Hereafter, we use the term deposition when referring to accumulation rates of the storm layer and differentiate this from burial, a term we use to refer to measurements made over decadal or longer timescales derived from ^{210}Pb measurements by previous research.

Respiration

Intact Cores

Duplicate intact cores (10-cm interior diameter × 25-cm depth) were collected from three random locations at each site for measurements of surface CO_2 fluxes. One of the duplicate cores included the surface storm sediment layer, while the other had the storm sediment layer and surface litter manually removed to reflect pre-storm soil conditions. Cores were stored in coolers on ice until return to the laboratory and were allowed to acclimate for 14 days (following soil disturbance and shearing of any roots during core collection and travel) under simulated tidal conditions in a well-ventilated facility on the campus of University of Central Florida before the first measurements were made.

Unfiltered surface water was collected from each site and was used to manually simulate tidal flooding in the cores. A single hole (0.64-cm diameter) was drilled into the base of each core to enable drainage; rubber stoppers were used to prevent drainage during simulated high tide conditions. Water was filled to a 2-cm depth above the soil surface three times each week and subsequently allowed to drain after 24 h. Soil CO_2 fluxes were measured using a LI-COR 8100 (LICOR Biosciences, Lincoln, NE) under flooded and exposed conditions twice a week for 4 weeks.

Bottle Incubations

Rates of potential soil respiration under anaerobic (i.e., inundated) conditions were measured with bottle incubations, and sequential headspace extractions were analyzed on a gas chromatograph. These measurements were conducted to assess whether there was a difference in the respiration potential of the separated storm and pre-storm soils (i.e., with no interaction between the two layers, as was present in the intact core design). Bottle microcosms were created by weighing approximately 5 g of homogenized, field-moist soil into 100-mL serum bottles that were sealed with a rubber septum and crimped aluminum cap. Each bottle was evacuated under vacuum and then purged with 99% O_2-free N_2 gas. Site water was filtered (0.45 μm) then purged with N_2 gas before 14 mL was injected into the bottles. Bottles were placed in an orbital shaker at 125 rpm and 25 °C. The headspace concentration of CO_2 was sampled with a glass, gas-tight syringe beginning 24 h after injection of the site water, and again at 48, 96, 144, and 216 h. Gas samples were measured using a GC-2014 Gas Chromatograph (Shimadzu Instruments, Kyoto, Japan) with a flame ionization detector and a Hayesep N 80/100 mesh 1/8 in. × 1.5 m stainless pre-conditioned column. Henry's law was used with measurements of headspace pressure and water pH to calculate the dissolved concentration of CO_2. The pH of the water used in the incubations was measured using an Accumet benchtop pH probe (Accumet XL200, Thermo Fisher Scientific, Waltham, MA, USA) after all headspace extractions were complete. The rate of efflux was calculated by linear regression of total bottle concentration (headspace + dissolved) as a function of time.

Gas fluxes from bottle incubation are generally reported on a mass basis (mg C kg soil^{-1} h^{-1}) while fluxes from the LICOR intact core measurements are reported on an areal basis (μmol CO_2 m^{-2} s^{-1}). In order to compare measurements from the two techniques, the mass fluxes from the bottle incubations were converted to an areal basis using the DBD of the soil.

Soil Microbial Properties

Analysis of soil samples for microbial biomass C (MBC) and extracellular enzyme activities began within 48 h of field collection. The chloroform fumigation extraction procedure (Vance et al. 1987) was used to measure MBC as the difference between fumigated and non-fumigated samples. Homogenized, wet soil samples of 2.5 g were weighed into duplicate sets of 40-mL centrifuge tubes. The first set was placed in a glass desiccator and exposed to gaseous chloroform within the headspace for 24 h. Afterwards, both fumigated and non-fumigated samples were filled with 25 mL 2 M KCl and then shaken for 1 h to suspend the soil in solution. Samples were subsequently centrifuged, decanted and vacuum filtered (0.45 μm), and then acidified for preservation. Measurement from both treatments was conducted using a Shimadzu TOC-L Analyzer (Kyoto, Japan). The DOC from the non-fumigated treatment represents extractable carbon (see "Soil Microbial Properties"). Microbial biomass C was calculated as the difference between fumigated and non-fumigated DOC divided by dry soil mass and multiplied by a k_{EC} factor of 2.22 (Joergensen 1996).

Assays of extracellular enzyme activities were performed using fluorescent 4-methylumbelliferone (MUF) for standardization and fluorescently labeled substrates (MUF) specific to each of the extracellular enzymes: β-1-4-glucosidase (GLUCO), β-D-xylopyranosidase (XYLO), and β-D-cellobiosidase (CELLO), as

indicators of C cycling, and β-N-acetylglucosaminidase (NAG), alkaline phosphatase (AP), and aryl sulfatase (SULF) as indicators of N, P, and S cycling, respectively (Chrost and Krambeck 1986; Hoppe 1993). A 1:78 slurry of soil to distilled, deionized water was created and shaken continuously at 25 °C in the dark for 1 h at 150 rpm to release the enzymes into solution. Fluorescently labeled MUF substrates were then added to an aliquot of the soil slurry and were read both immediately and after 24 h on a BioTek Synergy HTX (BioTek Instruments, Inc., Winooski, VT, USA) using excitation/emission wavelengths of 360/460. Enzyme activities were calculated as converted units of fluorescence to moles per gram of dry soil per hour (Bell et al. 2013).

Extractable Nutrient Concentrations

Extractable nutrients include the porewater concentrations as well as nutrients that are ionically complexed with soil particles. These were measured by liberating the nutrients from the soil complexes following the addition of KCl salts. The measured nutrients were dissolved organic carbon (DOC), NO_3^-, NH_4^+, and orthophosphate (PO_4^{3-}) hereafter referred to as soluble reactive phosphorus (SRP) for the inorganic form of P available for plant utilization. Extractable NO_3^- and NH_4^+ were combined and reported as extractable dissolved inorganic N (DIN). Colorimetric analysis of samples was conducted with a SEAL AQ2 Automated Discrete Analyzer (Seal Analytical, Mequon, WI) using EPA Methods 353.2 Rev. 2.0, 350.1 Rev. 2.0, and 365.1 Rev. 2.0, respectively, for NO_3^-, NH_4^+, and PO_4^{3-} (USEPA 1993).

Data Analyses

Statistical analyses were conducted within both IBM SPSS Statistics Version 25 and R 3.4.0 in R Studio (1.0.143) (R Foundation for Statistical Computing, Vienna, Austria). Comparisons of the Irma deposition rates between the three sites were conducted with a one-way ANOVA and post-hoc Tukey tests ($\alpha = 0.05$). Comparisons of the storm and pre-storm soil characteristics were made using two separate statistical tests: between sites (grouped by soil layer) and between soil layers (within sites). The Shapiro-Wilk test was applied to each parameter, subset by site, to determine normality. Those parameters that did not meet the assumptions of normality were transformed. Following transformations, Welch's t test was performed to determine differences between the storm and pre-storm soil within each site. The respiration data from the intact soil cores was analyzed using a paired t test between soil layers within each site. Prior to determining significance between sites (grouped by soil layer), Levene's test was used to verify assumptions of homogeneity of variance. Due to spatial variability within the sites, multiple parameters did not meet this assumption. Thus, a weighted linear regression

was used to account for the heteroscedasticity within each dataset, where the weight was defined by the reciprocal of the residuals derived from the null model (linear regression with site as a predictor variable) squared. If site was a significant predictor variable within the weighted linear regression, a post-hoc least squared means test was performed to further determine significance (package lsmeans). A Bonferroni correction (α/c; where c is the number of comparisons performed) was applied due to the multiple comparisons conducted, resulting in a corrected significance level of $\alpha = 0.025$. All reported values are untransformed and all uncertainties hereafter represent one standard error (S.E.), unless otherwise stated.

Results

Deposition from Hurricane Irma

The average sediment accretion following Hurricane Irma was highest nearest the GOM at SRS-7b (4.31 ± 0.11 cm), with a slight decrease at sites SRS-6 and SRS-5 (3.02 ± 0.12 cm and 3.29 ± 0.29, respectively) (Fig. 2a, b; Table 1). There was substantial spatial variability at SRS-5, which included both the lowest and highest individual measurements of storm accretion at all three sites (2.4 and 4.9 cm).

The mass of sediment deposition was highest at SRS-7b (31.5 ± 2.4 kg m^{-2}) with sites SRS-6 and SRS-5 having only approximately half that amount (18.2 ± 0.9 and 14.4 ± 1.2 kg m^{-2}, respectively) (Fig. 2c). This pattern of highest deposition at SRS-7b and lower rates at SRS-6 and SRS-5 was similar for all other deposition measurements, with the exception of OC deposition, which was not statistically different between the three sites (Fig. 2d; Table 1). Calcium carbonate made up the majority of sediment mass in the storm deposits, decreasing from 19.0 ± 1.6 kg m^{-2} at site SRS-7b to 7.3 ± 0.9 kg m^{-2} at SRS-5 (Fig. 2c). Organic matter was less than a third of total mass deposition, but still substantial, decreasing from 4.6 ± 0.1 kg m^{-2} at SRS-7b to 2.9 ± 0.1 kg m^{-2} at SRS-5.

Table 1 Statistical results for comparisons of Hurricane Irma's deposition by site (Fig. 2). Significance levels are indicated by * ($p \leq 0.05$), ** ($p < 0.01$), *** ($p < 0.001$), and ns (not significant; $p > 0.05$)

Parameter	df	F	Significance
Accretion	2, 6	24.8	**
Mass	2, 6	29.6	**
CaCO$_3$	2, 6	31	**
Soil organic matter	2, 6	51.8	***
Organic carbon	2, 6	4.1	ns
Inorganic carbon	2, 6	71.1	***
Total nitrogen	2, 6	34.4	**
Total phosphorus	2, 6	35.8	***

Because of the high $CaCO_3$ content, IC deposition was higher than OC deposition at all three sites, decreasing from 6.3 ± 0.5 to 1.6 ± 0.1 kg m^{-2} from SRS-7b to SRS-5. There was no difference in OC deposition across sites (Fig. 2d; Table 1, $p = 0.08$), with a regional average of 1.1 ± 0.1 kg m^{-2}. Deposition of both TN and TP was highest at SRS-7b (93.1 ± 0.9 and 17.0 ± 1.0 g m^{-2}, respectively) and lowest at SRS-5 (62.9 ± 1.5 and 8.1 ± 1.2 g m^{-2}, respectively) (Fig. 2e, f).

Physical Characteristics and Composition of Storm and Pre-storm Soils

The physical characteristics and composition of both the storm and pre-storm soils were not homogenous across sites. Differences were identified within both layers across sites for DBD, $CaCO_3$, and DIN (Fig. 3a, e, j). Mean DBD of the storm layer decreased from 0.73 ± 0.03 g cm^{-3} at site SRS-7b to 0.44 ± 0.04 g cm^{-3} at SRS-5 (Fig. 3a). For the pre-storm soils, the difference between sites was even more substantial, decreasing from 0.69 ± 0.03 g cm^{-3} at SRS-7b to 0.11 ± 0.01 g cm^{-3} at SRS-5 (Fig. 3a). Similarly, the $CaCO_3$ content of the storm layer was higher at site SRS-7b ($60 \pm 1\%$) compared to SRS-5 ($50 \pm 4\%$), while in the pre-storm soils, the $CaCO_3$ content decreased from 58 ± 1 to $5 \pm 0.2\%$ (Fig. 3e).

Spatial patterns were not as clear for DIN, with the highest concentrations in the Irma layer occurring at SRS-6 (4.4 ± 0.6 mg kg soil^{-1}) and the lowest concentrations at SRS-5 (1.9 ± 0.1 mg kg soil^{-1}) (Fig. 3j). In the pre-storm layer, the highest DIN concentrations occurred at SRS-5 and the lowest concentrations at SRS-6 (6.7 ± 0.8 and 1.3 ± 0.2 mg kg soil^{-1}, respectively) (Fig. 3j).

For all the remaining soil characteristics, there were no differences between sites within the storm layer ($p > 0.025$); within the pre-storm soil, often only site SRS-5 was different, with the exception of SOM and TP (Fig. 3; Table 2). For pre-storm SOM, there was a difference between the three sites, increasing from $17 \pm 1\%$ at SRS-7b to $65 \pm 1\%$ at SRS-5 (3b). For pre-storm soil TP, the concentration increased from 0.54 ± 0.01 mg g^{-1} at SRS-7b to 0.78 ± 0.08 mg g^{-1} at SRS-5 (Fig. 3h).

There were no differences between the storm and pre-storm soils at site SRS-7b for all soil characteristics and extractable nutrients measured in this study (Fig. 3; Table 2). For sites SRS-6 and 5, the differences between the storm and pre-storm soils were significant for all soil characteristics except MBC (Fig. 3; Table 2). In general, the differences between the soil layers were most pronounced at site SRS-5 where the gray storm sediment layer of high DBD and high $CaCO_3$ content
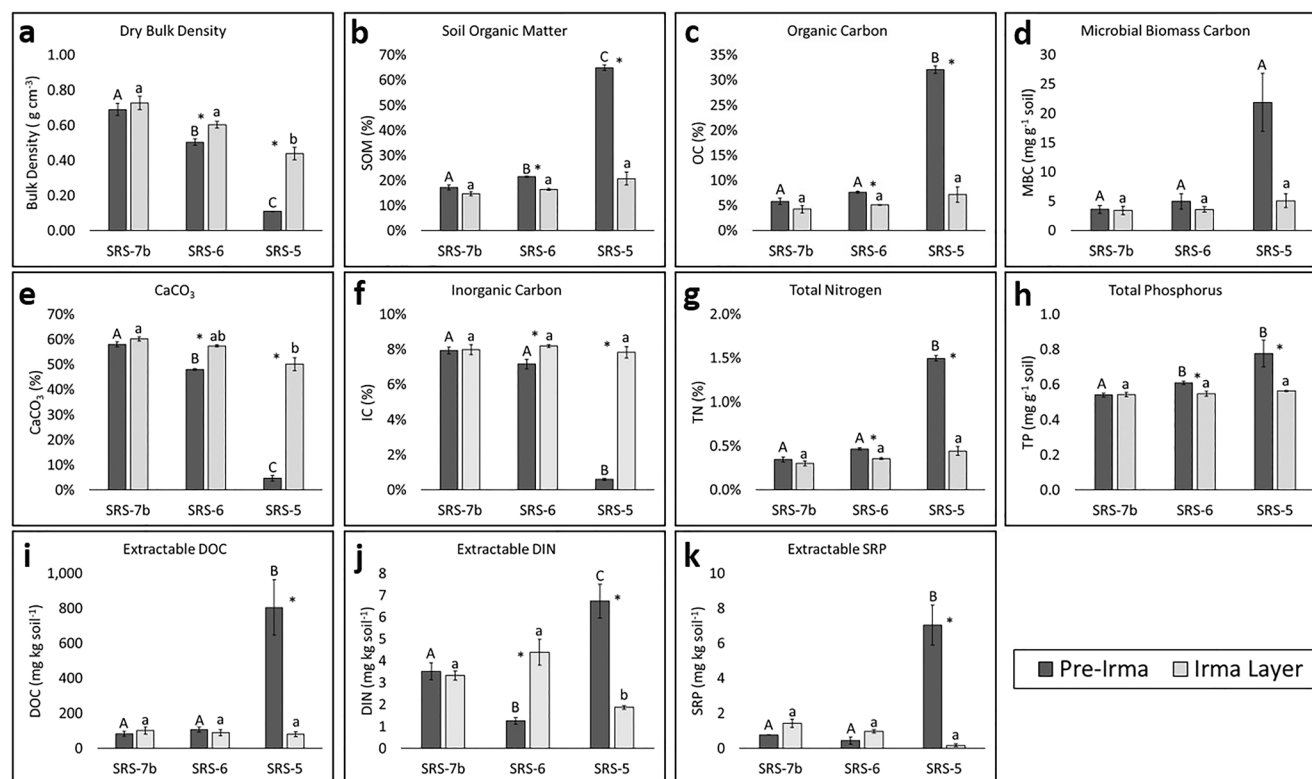

Fig. 3 Mean (± 1 SE) values of pre-Irma and Irma layer soils by site for **a** dry bulk density, **b** soil organic matter, **c** organic carbon, **d** microbial biomass carbon, **e** $CaCO_3$, **f** inorganic carbon, **g** total nitrogen, **h** total phosphorus, **i** extractable dissolved organic carbon (DOC), **j** extractable dissolved inorganic nitrogen (DIN), and **k** extractable soluble reactive phosphorus (SRP). Different capital letters indicate significant difference for pre-Irma soils by site; different lowercase letters indicate significant difference for Irma layer soils by site, and asterisks indicate significant difference between pre-Irma and Irma soils within a site. Statistical significance results are provided in Table 2

Table 2 P-values obtained from weighted linear regression model for between-site contrasts of storm and pre-storm soils and Welch's two sample t-test for within site contrasts for each parameter tested. Significance levels are indicated by * (p≤0.025), ** (p<0.01), *** (p<0.001) and ns (not significant; p>0.025). For within site soil respiration comparisons * indicates p≤0.05 and ns indicates p>0.05. Transformations that were used to meet conditions of normality include reciprocal (1/x) or logarithmic (Log₁₀(1+x)).

Parameter	Within soil type comparisons by site: Pre-Storm Soil			Within soil type comparisons by site: Storm Soil			Within site comparisons by soil type: Storm vs. Pre-Storm			Transformation Used
	7b vs. 6	6 vs. 5	7b vs. 5	7b vs. 6	6 vs. 5	7b vs. 5	7b	6	5	
Soil Characteristics (Fig. 3)										
Dry bulk density	**	***	***	ns	*	**	ns	*	***	None
Soil organic matter	*	***	***	ns	ns	ns	ns	**	**	Reciprocal
Calcium carbonate	**	***	***	ns	ns	**	ns	***	***	None
Organic carbon	***	***	ns	ns	ns	ns	ns	***	*	Reciprocal
Inorganic carbon	ns	ns	ns	ns	ns	ns	ns	*	***	None
Total nitrogen	ns	ns	**	ns	ns	ns	ns	**	**	Reciprocal
Total phosphorus	**	ns	*	ns	ns	ns	ns	*	*	Reciprocal
Microbial biomass carbon	ns	ns	ns	ns	ns	ns	ns	ns	ns	None
Extractable Nutrients (Fig. 3)										
Dissolved organic carbon	ns	**	*	ns	ns	ns	ns	ns	*	Reciprocal
Inorganic nitrogen	**	**	*	ns	**	**	ns	**	**	None
Soluble reactive phosphate	ns	**	***	ns	ns	ns	ns	ns	**	Logarithmic
Soil Respiration (Fig. 4)										
Anaerobic bottles (mass basis)							ns	ns	**	Reciprocal
Anaerobic bottles (area basis)							ns	ns	*	Reciprocal
Intact cores (flooded)							ns	ns	ns	None
Intact cores (exposed)							ns	ns	*	None
Enzyme Activities (Fig. 5)										
XYLO	ns	ns	ns	ns	ns	ns	ns	ns	ns	Reciprocal
CELLO	ns	ns	ns	ns	**	*	ns	*	ns	Reciprocal
GLUCO	ns	ns	ns	ns	ns	ns	ns	ns	ns	Reciprocal
NAG	ns	***	*	ns	ns	***	ns	ns	ns	Reciprocal
AP	ns	ns	ns	ns	***	***	*	**	ns	Logarithmic
SULF	ns	ns	ns	ns	ns	ns	**	ns	ns	None

was contrasted by the dark brown peat with low DBD and high SOM content in the underlying soil (Fig. 2a). Overall, the peat soil at SRS-5 was uniquely different from all other soils, having the lowest DBD (0.11 ± 0.00 g cm^{-3}), CaCO$_3$ ($4.7 \pm 0.2\%$), and IC ($0.6 \pm 0.1\%$) (Fig. 3a, e, f) and the highest soil concentration of SOM ($64.9 \pm 1.1\%$), OC ($32.3 \pm 0.1\%$), MBC (9.9 ± 2.2 mg kg soil^{-1}), TN ($1.5 \pm 0.0\%$), and TP (0.78 ± 0.08 mg g^{-1}) (Fig. 3b, c, d, g, h).

Soil Respiration

The average flux of CO_2 from the aerobic intact cores ranged from a low of 1.08 ± 0.14 μmol m^{-2} s^{-1} for the soils that included the storm layer at SRS-6 to a high of 2.43 ± 0.19 μmol m^{-2} s^{-1} for the cores without a storm layer at SRS-5. This high flux from the pre-storm soil cores at SRS-5 was greater than the mean flux from the intact cores with a storm layer present from the same site and supports our third hypothesis (Fig. 4a; Table 2). There was no difference in mean respiration rates between the storm and pre-storm soils at the other two sites. The atmospheric flux of CO_2 from intact cores under anaerobic, flooded conditions was substantially lower than the rates measured under aerobic conditions. Average fluxes were

similar between sites and treatments and ranged from a low of 0.47 ± 0.07 μmol CO_2 m^{-2} s^{-1} for the cores that included the storm layer of SRS-6 to a high of 0.81 ± 0.16 μmol CO_2 m^{-2} s^{-1} for the pre-storm soil cores at SRS-6 (Fig. 4b).

The average CO_2 fluxes for the anaerobic bottle incubations ranged from a low of 0.26 ± 0.01 mg CO_2-C kg soil^{-1} h^{-1} for the pre-Irma layer at SRS-7b to a high of 8.4 ± 1.7 mg CO_2-C kg soil^{-1} h^{-1} for the pre-Irma soil at SRS-5 (Fig. 4c). Of the three sites, there was only a difference in potential respiration between the soils at site SRS-5, where the rate from the pre-storm soil was 11 times higher than from the storm layer. When the bottle fluxes were normalized for DBD and stated on an areal basis the fluxes ranged from a low of 0.04 ± 0.00 μmol CO_2 m^{-2} s^{-1} for the pre-storm layer at SRS-7b to a high of 0.21 ± 0.04 μmol CO_2 m^{-2} s^{-1} for the pre-storm soil at SRS-5. There was only a difference between the potential respirations of the soils for site SRS-5 (Fig. 4d; Table 2). The overall mean of the anaerobic bottle fluxes expressed on an areal basis was 0.10 ± 0.02 μmol CO_2 m^{-2} s^{-1} (Fig. 4d), which is approximately six times lower than the mean of the anaerobic intact core fluxes (0.61 ± 0.04 μmol CO_2 m^{-2} s^{-1}).

Fig. 4 Mean (± 1 SE) CO_2 fluxes from **a** intact cores under low tide/ exposed to the atmosphere, **b** intact cores under high tide/flooded conditions, and anaerobic bottle incubations reported on a **c** per mass basis and **d** per area basis (note different scale of *y*-axis). The intact cores are either composed exclusively of pre-Irma soil or of a combination of pre-Irma soil capped by an Irma layer. The bottle incubations are composed exclusively of pre-Irma or Irma soil only. Asterisks indicate a significant difference ($p < 0.05$) between treatments within a site. Statistical significance is reported in Table 2
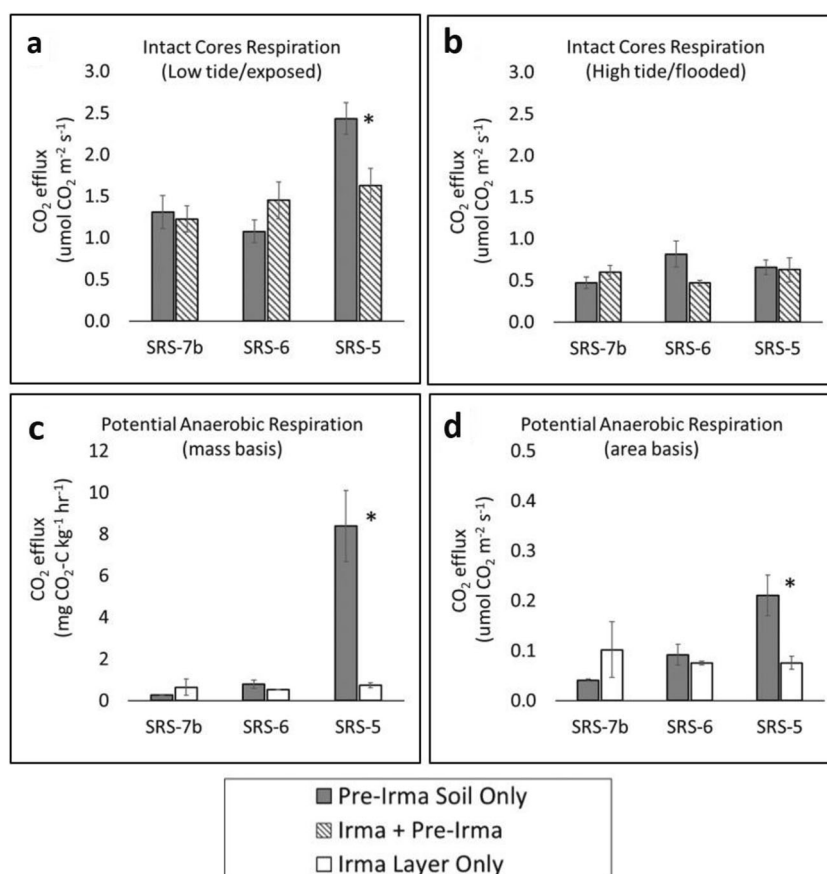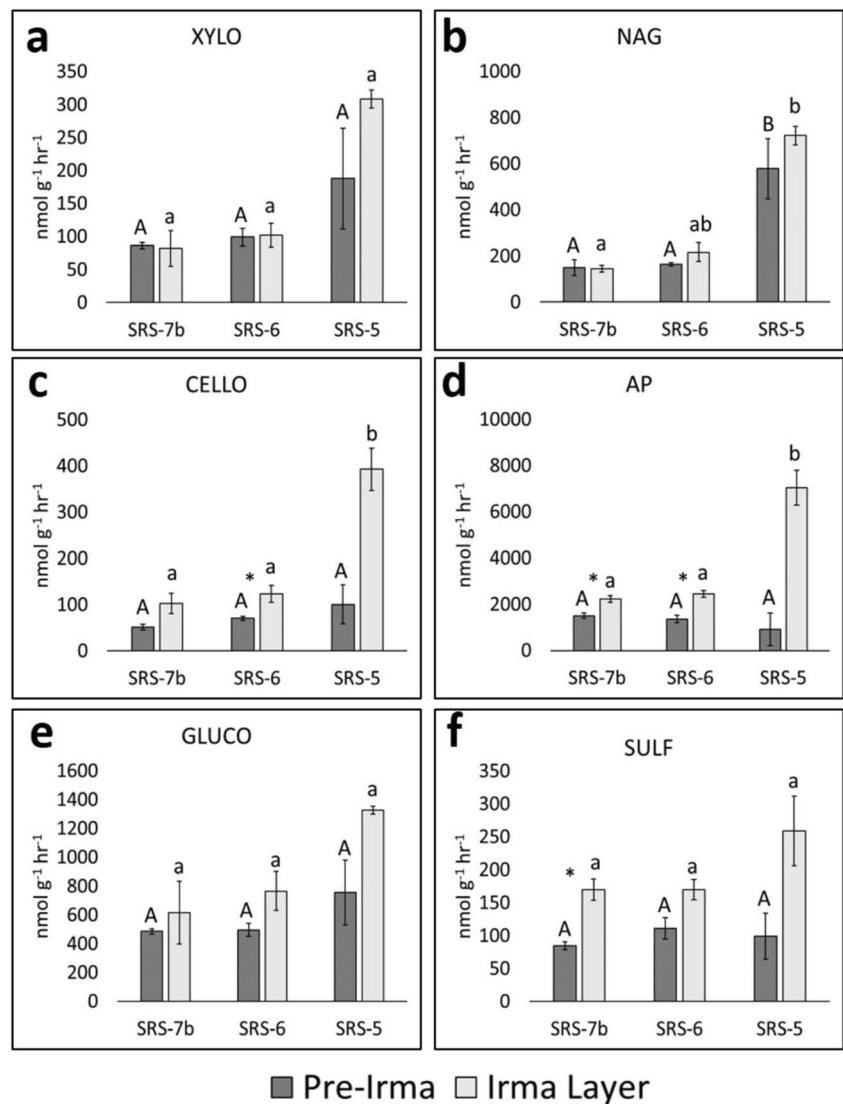
Fig. 5 Mean (± 1 SE) extracellular enzyme activities for pre-Irma and Irma soils by site for **a** β-D-xylopyranosidase (XYLO), **b** β-N-acetylglucosaminidase (NAG), **c** β-D-cellobiosidase (CELLO), **d** alkaline phosphatase (AP), **e** β-1-4-glucosidase (GLUCO), and **f** aryl sulfatase (SULF). Different capital letters indicate significant difference for pre-Irma soils by site; different lowercase letters indicate significant difference for Irma layer soils by site, and asterisks indicate significant difference between pre-Irma and Irma soils within a site. Statistical significance results are provided in Table 2

Soil Microbial Biomass and Extracellular Enzyme Activities

Microbial biomass carbon ranged from a low of 3.4 ± 0.7 mg g soil^{-1} in the storm layer at SRS-6 to a high of 9.86 ± 2.21 mg g soil^{-1} in the pre-storm soil at SRS-5. However, high variability in the replicates prevented detection of significant differences between the soils both within and between sites (Fig. 3d; Table 2).

Extracellular enzyme activities trended higher (though not always significantly) in the storm layer compared to the pre-storm soils and in the upstream sites (Fig. 5). Activities of CELLO, AP, and SULF all showed differences between the soils, though not for all sites (Fig. 5c, d, f; Table 2). High variability prevented identification of differences for a number of enzyme activities; XYLO, GLUCO, and NAG were the same in both soils at all three sites.

Discussion

Respiration Suppression

The presence of the Irma layer suppressed efflux of CO_2 to the atmosphere from the unflooded intact cores by 30% compared to soil from the same site without the overlying storm layer (Fig. 4a), supporting our third hypothesis. This suppression effect was only observed at site SRS-5 where the pre-storm soil was highly organic (Fig. 3b) and supported higher potential respiration rates than the pre-storm soils at the other sites (Fig. 4c). Two possible reasons for the decreased efflux could be (1) the high DBD storm layer acted as a physical barrier that prevented the efflux of gas from the underlying organic soil to the atmosphere (and simultaneously prevented the influx of O_2 from the atmosphere) or (2) the change in physicochemical properties (i.e., decreased OC content) of the surficial, biogeochemically active layer. A regression of the total

OC stock versus respiration of each of the intact cores ($n = 18$) showed that OC stock was not a significant predictor ($r^2 = 0.16$; $p = 0.097$) of a core's CO_2 flux. It should be noted that this relationship might be more predictive if the total OC pool was separated into labile and refractory components. We propose that the high-density storm layer physically caps the underlying soil, inhibiting interaction with the atmosphere and potentially enhancing anaerobic conditions in the underlying soils. In fine-grained soils with high water holding capacity, the depth of oxygen penetration occurs on the scale of only a few millimeters (Green and Aller 1998; DeLaune and Reddy 2008). This is consistent with the observation that typhoon Chan-hom caused mangrove soils to become more anoxic after the storm's occurrence (Salmo et al. 2014). Similarly, Eh values decreased following thin layer placement of dredged material (up to 10 cm thick) on the surface of a restored wetland (Croft et al. 2006). It should also be noted from the example of typhoon Chan-hom referenced above that soil redox conditions returned to pre-storm levels within 7 months of the storm (Salmo et al. 2014), providing evidence that although storm alterations to biogeochemical cycling can be considerable, they are not likely to be permanent. Furthermore, although the storm layer prevented the flux of CO_2 from the soil to the atmosphere, it is also possible that CO_2 from microbial respiration in the underlying soil was exported from the soil as dissolved inorganic carbon (DIC).

Rates of Accretion and Deposition of Carbon and Nutrients

Sediment accretion from this single event (3.0–4.3 cm) was roughly equal to the annual average accretion rate throughout the previous 10 years (3.5 ± 0.5 mm year^{-1} for SRS-5, and 3.5 ± 1.3 mm year^{-1} for SRS-6 and SRS-7b) and substantially higher than the annual average over the past century (2.4 ± 0.4 mm year^{-1} for SRS-5 and 2.2 ± 0.4 mm year^{-1} for SRS-6 and SRS-7b) (Breithaupt et al. 2017). The addition of this material is a valuable mechanism for these wetlands to maintain pace with the regional rate of relative sea-level rise, which has averaged 2.42 mm year^{-1} since 1913 and has increased to 8.1 ± 1.6 mm year^{-1} in the last decade (NOAA National Ocean Service 2018). Gains in accretion do not necessarily produce corresponding elevation increases because pre-storm peat soils may be susceptible to auto-compaction from the additional overburden of the storm layer's mass (Breithaupt et al. 2017) or if tree mortality due to the storm leads to root zone collapse (Cahoon 2006; Whelan et al. 2009). Over time, the storm layer will be altered through natural processes, such as rainfall-driven erosion, crab burrow construction, and ingrowth of roots (Whelan et al. 2009). Nonetheless, storm

deposition represents a substantive addition to the soil body with impacts on biogeochemical cycling.

The storm layer also represents a significant addition of organic carbon and nutrients to the soil, supporting our first hypothesis (Fig. 2). Irma's deposition of OC was 7–10 times greater than the average annual rate for the past century determined using ^{210}Pb dating (Breithaupt et al. 2014). Similarly, TN deposition from this storm was 9–15 times higher and TP deposition was 17–22 times higher than the previous 100-year averages at these sites. These added nutrients can relieve nutrient limitation stress in carbonate platform mangroves that receive very little terrigenous inputs and normally rely on efficient internal cycling in order to attain sufficient nutrients (McKee 2001).

It may seem paradoxical that the addition of storm sediment, with roughly 80–85% mineral $CaCO_3$ content, also contributes to such high burial rates of SOM and OC. This is explained by the storm layer's high bulk density: a large mass is compressed into a given volume. Therefore, while the percentage of SOM or OC is relatively low compared to the total mineral or $CaCO_3$ content in the storm layer (Fig. 3), the higher bulk density relative to the underlying soils equates to an overall increase in these constituents. For the purpose of this comparison, it is important to note that the DBD of the pre-storm soils (Fig. 3a) represents only the first 5 cm of soil below the Irma layer and is roughly two times greater than the average dry bulk density reported for the first 40 cm of soil by Breithaupt et al. (2017) at these same sites. The contrast between the soils at sites SRS-6 and 7b is not as distinct because the first 0–10 cm of the pre-Irma soil likely still includes storm sediment from Hurricane Wilma (2005). The lack of substantial differences between the soils (Fig. 3) suggests that the sites nearest the coast receive a more regular supply of carbonate material during tidal events and not just during hurricanes and storm surges.

Sources and Stability of Organic and Inorganic Carbon

Soil OC represented $55.7 \pm 0.5\%$ of the total SOM across sites ($r^2 = 0.9986$) (Fig. 6a). This relationship is roughly 10% higher than the value of $42.4 \pm 1.4\%$ that has been reported for a broad range of south Florida mangrove soils (Radabaugh et al. 2018) and 41.5% reported for mangrove soils in the Republic of Palau (Kauffman et al. 2011). With the exception of the pre-storm peat soil at SRS-5, the organic matter in these soils is mostly composed of litter rather than roots, and because the SOM in the storm soils is less than 20% of soil mass (Fig. 3b), its scarcity makes it a more valuable resource for microbial respiration. The higher than usual relationship of OC:SOM may be because this SOM has undergone a greater degree of decomposition resulting in a higher ratio of OC:TN. Microbial biomass carbon represented $6.6 \pm 0.8\%$ of the
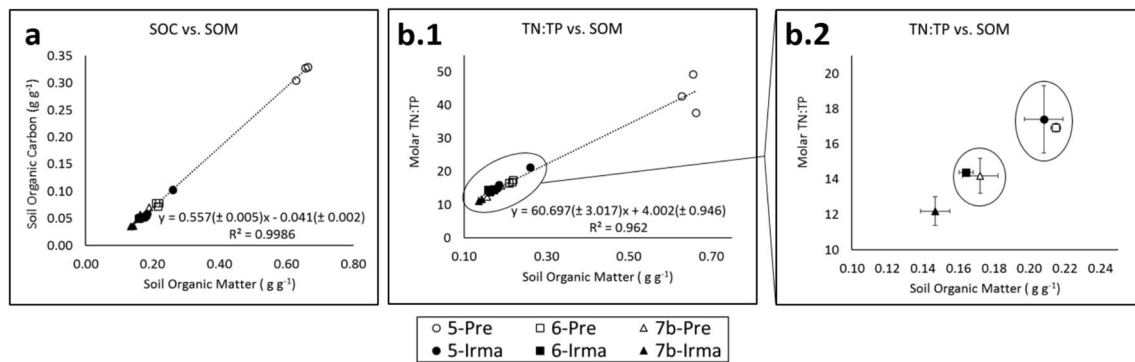
Fig. 6 Linear regressions for (a) soil organic carbon (SOC) as a function of soil organic matter (SOM), (b.1) molar TN:TP as a function of SOM, and (b.2) mean (± 1 SE) for a subset of panel (b.1) showing the grouping of the Irma and pre-Irma soils from different sites

total soil OC pool across sites and soil types ($r^2 = 0.7978$). This value is on the high end of MBC:OC values reported in the literature (Dalal 1998) and suggests relatively intense biogeochemical activity. However, while there was a positive correlation between MBC and anaerobic soil respiration in the incubation bottles ($r^2 = 0.9351$), the slope of 0.41 (rather than 1.0) indicates that increases in MBC do not correspond to proportional losses of soil carbon via respiration. This suggests that much of microbial activity in these soils involves transforming soil constituents rather than mineralization.

The Irma sediment layer represents the addition of 1.1–2.5 kg m^{-2} of particulate IC to these mangrove soils (Fig. 2d). These values are substantially higher than twentieth century average IC burial rates in mangroves of the Central Red Sea region (290 ± 120 g IC m^{-2} year^{-1}) and Arabian Gulf (230 ± 180 g IC m^{-2} year^{-1}), regions where carbonate sediments represent 40–60% of soil volume (Saderne et al. 2018). The large influx of IC raises the question of how it affects the regional carbon budget (Troxler et al. 2013). As Macreadie et al. (2017) have discussed, the role of IC in coastal carbon budgets is complicated by substantial uncertainties related to (1) its provenance (i.e., is it of recent biogenic origin or is it old and geogenic in origin?), (2) its stability (i.e., is it susceptible to dissolution from ocean acidification or sea-level rise), and (3) whether there are linkages between OC and IC burial rates. In the circumstance of large storms delivering carbonate mud into the mangrove forests, these questions are highly relevant. First, because the carbonate mud is delivered during storms, its provenance can reliably be stated as coming from the GOM. Therefore, while formation/precipitation of carbonate is a net source of CO_2, that flux should be accounted for elsewhere in the marine environment. Secondly, IC stability in these mangrove soils could potentially be limited if conditions are favorable for $CaCO_3$ dissolution. The occurrence of occasionally acidic conditions that could be favorable for carbonate dissolution has been observed at sites SRS-5 and SRS-6. Over the past 18 years of surface water pH measurements at SRS-5, 53% of the values ($n = 73$) were less than 6.5 and 15%

were less than 6.0; at SRS-6, 32% of measurements ($n = 76$) were less than 6.5 and 5% were less than 6.0 (Castañeda and Rivera-Monroy 2018). Dissolution of carbonate has the net effect of removing CO_2 from the atmosphere, and therefore, its occurrence would have the potential to increase the regional C sink capacity of these wetlands.

Enzyme Activities

Activities of extracellular enzymes like GLUCO, CELLO, AP, and SULF have all been observed to positively correlate with soil organic content (Makoi and Ndakidemi 2008 and references therein); however, no such correlation was found for these data ($p > 0.05$). Instead, enzyme activities in the Irma layer were equal to or greater than activities in the pre-storm soil (Fig. 5). This indicates additional environmental drivers such as altered redox, salinity, and moisture conditions are also influencing rates of extracellular enzyme synthesis. For example, if the storm layer contributed to decreased soil CO_2 effluxes by creating more reduced conditions in the underlying soil ("Respiration Suppression"), then it likely had a dampening effect on enzyme production as well.

Of the six enzymes analyzed here, the greatest number of differences between soil layers and sites was found for AP, with higher activities detected in the storm layer compared to the pre-storm soils. As noted earlier, the storm layer may create more reduced conditions in the underlying soils and thus be a mechanism for decreased enzyme activities; however, this does not explain the difference in AP activity between sites. According to evolutionary-economic principles, microbiota and plants excrete enzymes in circumstances where the desired resource is scarce (Koch 1985; Allison et al. 2011). Because the Everglades is P-limited, it might be expected that AP activity would negatively correlate with SRP, a biologically available form of P. There was no correlation between SRP and AP across all three sites ($r = -0.434$; $p = 0.072$), but there was a negative correlation within the samples at SRS-5 ($r = -0.933$, $p = 0.007$; $n = 6$) where there was the greatest contrast

between the soils. This negative correlation (i.e., highest AP activity occurring in the samples with the lowest SRP) likely occurs because microbiota do not need to excrete enzymes to utilize already mineralized end-products (Allison and Vitousek 2005) such as SRP.

For sites SRS-7b and SRS-6, the driver of AP activity appears to be different. There were no differences in extractable SRP between the soils at these sites (Fig. 5d), and the concentrations were much lower than in the pre-storm layer at SRS-5 (Fig. 3k). Instead, AP activities were negatively correlated with SOM content ($r = -0.710$; $P = 0.010$; $n = 12$), which directly contradicts previous observations of a positive correlation (Makoi and Ndakidemi 2008 and references therein). For these sites, the evolutionary-economic scarcity principle suggests that in the absence of available SRP, SOM is a limiting resource for microbial activity in the storm layer.

Spatial Variability of Soil Composition

The composition of the sediment in the Irma layer was not homogeneous across the landscape, indicating that the storm surge does not deposit a single sediment source equally across the region. Evidence of this is seen in the changing composition of the material vertically within the sites and laterally with distance from the GOM. Soil OM content was a strong predictor of regional nutrient limitation, with a positive relationship between TN:TP and SOM ($r^2 = 0.962$; Fig. 6(b.1)) and distinct groupings showing similarities between the Irma layer of one site and the pre-Irma soil at the site downstream from it (Fig. 6(b.2)). These observations lead to a speculative hypothesis about the process by which the storm surge acquired and deposited sediment spatially within the region (Fig. 7). According to this hypothesis, as storm surge moved ashore, it eroded surface sediment from the seaward wetlands and deposited that sediment in more

landward locations. As a result, SRS-5, the most upstream of our sites, received its storm sediment from the region of SRS-6; SRS-6 received its storm layer from the region of SRS-7b, and SRS-7b received its storm layer from a downstream location (Fig. 7). The transgressive process illustrated in this single storm event is likely a temporal microcosm of the general marine transgression occurring across the region because of sea-level rise (Spackman et al. 1966).

Conclusions

Our findings demonstrate that storms can provide large subsidies of carbon and nutrients through storm surge sediment deposition that would otherwise require several years to accumulate. Deposition of IC was greater than OC at all sites. Questions related to the origins of this IC and how stable it is are important to consider for regional carbon accounting. There were few physicochemical or biogeochemical differences between the storm and pre-storm soil layers at two of our sites closest to the GOM. This suggests a relatively frequent influence of marine sedimentation in the formation of the soils at these sites. However, at the site 8 km from the GOM, there were numerous differences between the two soil layers including DBD, SOM, MBC, IC, TN, TP, extractable nutrients, and potential respiration rates. Additionally, there were differences that occurred as a result of the interaction of the two soils including a decrease in atmospheric CO_2 efflux from soils with a storm layer, as well as generally lower enzyme activities in the pre-storm soils.

Wetlands with storm-damaged mangroves will likely have reduced productivity in the subsequent months or years as new recruitment occurs and they recover from defoliation. However, some of this decrease in CO_2 fixation may be offset by the storm sediment capping and preventing efflux of CO_2,

Fig. 7 Spatial conceptual model hypothesizing the landward transgressive process by which storm surge acquires and deposits marine sediments throughout the coastal Everglades
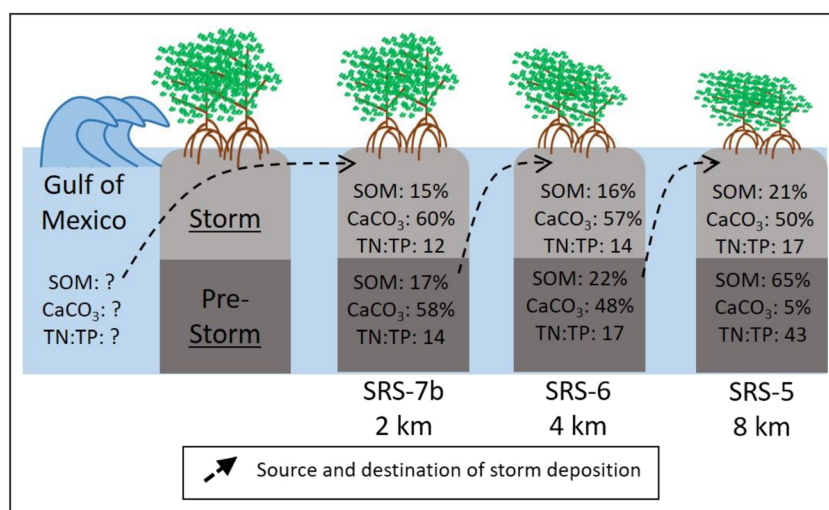
particularly in soils with high SOM content that are isolated from regular tidal deposition. More work across broader spatial and temporal scales would be useful to constrain the extent of this storm layer capping effect. Our observations suggest that sea-level rise along with large storms are likely to increase the deposition of this marine storm sediment within mangroves and eventually the brackish and freshwater marshes of coastal wetlands. The result of this marine transgression has the potential to aid in the preservation of historically sequestered soil carbon and avoid its loss through respiration.

References

Allison, Steven D., and Peter M. Vitousek. 2005. Responses of extracellular enzymes to simple and complex nutrient inputs. *Soil Biology and Biochemistry* 37 (5): 937–944. https://doi.org/10.1016/j.soilbio.2004.09.014.

Allison, Steven D., Michael N. Weintraub, Tracy B. Gartner, and Mark P. Waldrop. 2011. Evolutionary-economic principles as regulators of soil enzyme production and ecosystem function. In *Soil enzymology*, ed. G. Shukla and A. Varma, 275–285. Berlin Heidelberg: Springer-Verlag. https://doi.org/10.1007/978-3-642-14225-3.

Andersen, J.M. 1976. An ignition method for determination of total phosphorus in lake sediments. *Water Research* 10: 329–331.

Arkema, Katie K., Greg Guannel, Gregory Verutes, Spencer A. Wood, Anne Guerry, Mary Ruckelshaus, Peter Kareiva, Martin Lacayo, and Jessica M. Silver. 2013. Coastal habitats shield people and property from sea-level rise and storms. *Nature Climate Change* 3 (10): 913–918. https://doi.org/10.1038/NCLIMATE1944.

Barr, Jordan G., Vic Engel, Thomas J. Smith, and José D. Fuentes. 2012. Hurricane disturbance and recovery of energy balance, CO2 fluxes and canopy structure in a mangrove forest of the Florida Everglades. *Agricultural and Forest Meteorology* 153. Elsevier B.V.: 54–66. https://doi.org/10.1016/j.agrformet.2011.07.022.

Bell, Colin W., Barbara E. Fricks, Jennifer D. Rocca, Jessica M. Steinweg, Shawna K. McMahon, and Matthew D. Wallenstein. 2013. High-throughput fluorometric measurement of potential soil extracellular enzyme activities. *Journal of Visualized Experiments* (81). https://doi.org/10.3791/50961.

Bouillon, Steven, Alberto V. Borges, Edward Castañeda-Moya, Karen Diele, Thorsten Dittmar, Norman C. Duke, Erik Kristensen, Shing Y. Lee, Cyril Marchand, Jack J. Middelburg, Victor H. Rivera-Monroy, Thomas J. Smith III, and Robert R. Twilley. 2008. Mangrove production and carbon sinks: a revision of global budget estimates. *Global Biogeochemical Cycles* 22 (2): 1–12. https://doi.org/10.1029/2007GB003052.

Breithaupt, Joshua L., Joseph M. Smoak, Thomas J. Smith, and Christian J. Sanders. 2014. Temporal variability of carbon and nutrient burial, sediment accretion, and mass accumulation over the past century in a carbonate platform mangrove forest of the Florida Everglades. *Journal of Geophysical Research, Biogeosciences* 119 (10): 2032–2048. https://doi.org/10.1002/2014JG002715.

Breithaupt, J.L., J.M. Smoak, V.H. Rivera-Monroy, E. Castañeda-Moya, R.P. Moyer, M. Simard, and C.J. Sanders. 2017. Partitioning the relative contributions of organic matter and mineral sediment to accretion rates in carbonate platform mangrove soils. *Marine Geology* 390: 170–180. https://doi.org/10.1016/j.margeo.2017.07.002.

Breithaupt, J.L., Smoak, J.M., Sanders, C.J. and Troxler, T.G. 2019. Spatial variability of organic carbon, CaCO₃ and nutrient burial rates spanning a mangrove productivity gradient in the coastal Everglades. *Ecosystems* 22 (4):844–858.

Cahoon, Donald R. 2006. A review of major storm impacts on coastal wetland elevations. *Estuaries and Coasts* 29 (6): 889–898. https://doi.org/10.1007/BF02798648.

Cahoon, Donald R., Philippe Hensel, John Rybczyk, Karen L. McKee, C. Edward Proffitt, and Brian C. Perez. 2003. Mass tree mortality leads to mangrove peat collapse at Bay Islands, Honduras after Hurricane Mitch. *Journal of Ecology* 91 (6): 1093–1105. https://doi.org/10.1046/j.1365-2745.2003.00841.x.

Cangialosi, J.P., Latto, A.S and Berg R. 2018. National Hurricane Center Tropical Cyclone Report: Hurricane Irma. *National Oceanic and Atmospheric Administration*: May, 30.

Castañeda-Moya E, Rivera-Monroy V. 2018. Abiotic monitoring of physical characteristics in porewaters and surface waters of mangrove forests from the Shark River Slough and Taylor Slough, Everglades National Park (FCE), South Florida from December 2000 to Present. Environmental Data Initiative. https://doi.org/10.6073/pasta/1f61bffd880b6c90d31d92f501bfe3be. Accessed March 8, 2018.

Castañeda-Moya, Edward, Robert R. Twilley, Victor H. Rivera-Monroy, Keqi Zhang, Stephen E. Davis, and Michael Ross. 2010. Sediment and nutrient deposition associated with Hurricane Wilma in mangroves of the Florida coastal everglades. *Estuaries and Coasts* 33 (1): 45–58. https://doi.org/10.1007/s12237-009-9242-0.

Chrost, R.J., and H.J. Krambeck. 1986. Fluorescence correction for measurements of enzyme-activity in natural-waters using methylumbelliferyl substrates. *Archive Fur Hydrobiologie* 106: 79–90.

Croft, Alex L., Lynn A. Leonard, Troy D. Alphin, and Lawrence B. Cahoon. 2006. The effects of thin layer sand renourishment on tidal marsh processes: Masonboro Island, North Carolina. *Estuaries and Coasts* 29 (5): 737–750.

Dalal, R.C. 1998. Soil microbial biomass—what do the numbers really mean? *Australian Journal of Experimental Agriculture* 38 (7): 649–665.

Danielson TM, Rivera-Monroy VH, Castañeda-Moya E, Briceño H, Travieso R, Marx BD, Gaiser E, Farfán LM. 2017. Assessment of Everglades mangrove forest resilience: Implications for aboveground net primary productivity and carbon dynamics. *For Ecol Manage* 404:115–125. https://doi.org/10.1016/j.foreco.2017.08.009

Dean, Walter E. 1974. Determination of carbonate and organic matter in calcareous sediments and sedimentary rocks by loss on ignition: comparison with other methods. *Journal of Sedimentary Research* 44: 242–248. https://doi.org/10.1306/74D729D2-2B21-11D7-8648000102C1865D.

DeLaune, Ronald D., and K. Ramesh Reddy. 2008. *Biogeochemistry of wetlands: science and applications*. CRC press.

Donato, Daniel C., J. Boone Kauffman, Daniel Murdiyarso, Sofyan Kurnianto, Melanie Stidham, and Markku Kanninen. 2011. Mangroves among the most carbon-rich forests in the tropics. *Nature Geoscience* 4. Nature Publishing Group: 293–297. https://doi.org/10.1038/ngeo1123.

Doyle, T.W., T.J. Smith, and M.B. Robblee. 1995. Wind damage effects of Hurricane Andrew on mangrove communities along the southwest coast of Florida, USA. *Journal of Coastal Research, SI* 21: 159–168.

Green, Mark A., and Robert C. Aller. 1998. Seasonal patterns of carbonate diagenesis in nearshore terrigenous muds: relation to spring phytoplankton bloom and temperature. *Journal of Marine Research* 56 (5): 1097–1123.

Harris, David, William R. Horwa, and Chris Van Kessel. 2001. Acid fumigation of soils to remove carbonates prior to total organic carbon or carbon-13 isotopic analysis. *Soil Science Society of America Journal* 65 (6): 1853–1856.

Hoppe, Hans-Georg. 1993. Use of fluorogenic model substrates for extracellular enzyme activity (EEA) measurement of bacteria. In *Handbook of methods in aquatic microbial ecology*, ed. Paul F. Kemp, Barry F. Sherr, Evelyn B. Sherr, and Jonathan J. Cole, 423–431. Boca Raton: CRC Press LLC.

Jennerjahn, Tim, and Venugopalan Ittekkot. 2002. Relevance of mangroves for the production and deposition of organic matter along tropical continental margins. *Naturwissenschaften* 89 (1): 23–30. https://doi.org/10.1007/s00114-001-0283-x.

Joergensen, Rainer Georg. 1996. The fumigation-extraction method to estimate soil microbial biomass: calibration of the Kec value. *Soil Biology & Biochemistry* 28 (1): 25–31.

Kauffman JB, Cole TG. 2010. Micronesian mangrove forest structure and tree responses to a severe typhoon. *Wetlands* 30:1077–1084.

Kauffman, J. Boone, Chris Heider, Thomas G. Cole, Kathleen A. Dwire, and Daniel C. Donato. 2011. Ecosystem carbon stocks of micronesian mangrove forests. *Wetlands* 31 (2): 343–352. https://doi.org/10.1007/s13157-011-0148-9.

Koch, A.L. 1985. The macroeconomics of bacterial growth. In *Bacteria in their natural environments*, ed. M. Fletcher and G.D. Floodgate, 1–42. London: Academic Press.

Krauss, Ken W., Thomas W. Doyle, Terry J. Doyle, Christopher M. Swarzenski, Andrew S. From, Richard H. Day, and William H. Conner. 2009. Water level observations in mangrove swamps during two hurricanes in Florida. *Wetlands* 29 (1): 142–149.

Long, Jordan, Chandra Giri, Jurgenne Primavera, and Mandar Trivedi. 2016. Damage and recovery assessment of the Philippines' mangroves following Super Typhoon Haiyan. *Marine Pollution Bulletin* 109. Elsevier Ltd: 734–743. https://doi.org/10.1016/j.marpolbul.2016.06.080.

Macreadie, Peter I., Oscar Serrano, Damien T. Maher, Carlos M. Duarte, and John Beardall. 2017. Addressing calcium carbonate cycling in blue carbon accounting. *Limnology and Oceanography Letters* 2 (6): 195–201. https://doi.org/10.1002/lol2.10052.

Maher, Damien T., Mitchell Call, Isaac R. Santos, and Christian J. Sanders. 2018. Beyond burial: lateral exchange is a significant atmospheric carbon sink in mangrove forests. *Biology Letters* 14 (7): 20180200. https://doi.org/10.1098/rsbl.2018.0200.

Makoi, Joachim H.J.R., and Patrick A. Ndakidemi. 2008. Selected soil enzymes: examples of their potential roles in the ecosystem. *African Journal of Biotechnology* 7: 181–191.

Mccoy, Earl D., Henry R. Mushinsky, Derek Johnson, and Walter E. Meshaka. 1996. Mangrove damage caused by Hurricane Andrew on the southwestern coast of Florida. *Bulletin of Marine Science* 59: 1–8.

Mckee, Karen L. 2001. Root proliferation in decaying roots and old root channels: a nutrient conservation mechanism in oligotrophic mangrove forests ? *Journal of Ecology* 89 (5): 876–887.

NOAA National Ocean Service. 2018. Mean sea level trend Key West Florida. Available from http://tidesandcurrents.noaa.gov/sltrends/sltrends_station.shtml?stnid=8724580. Accessed 29 Oct 2018

Radabaugh, Kara R., Ryan P. Moyer, Amanda R. Chappel, Christina E. Powell, Ioana Bociu, Barbara C. Clark, and Joseph M. Smoak. 2018. Coastal blue carbon assessment of mangroves, salt marshes, and salt barrens in Tampa Bay, Florida, USA. *Estuaries and Coasts* 41: 1496–1510. https://doi.org/10.1007/s12237-017-0362-7.

Radabaugh, K. R., Moyer, R. P., Chappel, A. R., Dontis, E. E., Russo, C. E., Joyse, K. M., Bownik, M. W., Goeckner, A. H. and Khan, N. S. 2019. Mangrove damage, delayed mortality, and early recovery following Hurricane Irma at two landfall sites in Southwest Florida, USA. *Estuaries and Coasts*. https://doi.org/10.1007/s12237-019-00564-8.

Roth, Linda C. 1992. Hurricanes and mangrove regeneration: effects of Hurricane Joan, October 1988, on the vegetation of Isla del Venado, Bluefields, Nicaragua. *Biotropica* 24 (3): 375–384.

Saderne, Vincent, Michael Cusack, Hanan Almahasheer, Oscar Serrano, Pere Masque, Ariane Arias-Ortiz, Periyadan Kadinjappalli Krishnakumar, Lotfi Rabaoui, Mohammad Ali Qurban, and Carlos Manuel Duarte. 2018. Accumulation of carbonates contributes to coastal vegetated ecosystems keeping pace with sea level rise in an arid region (Arabian Peninsula). *Journal of Geophysical Research, Biogeosciences* 123. https://doi.org/10.1029/2017JG004288.

Salmo, Severino G., Catherine E. Lovelock, and Norman C. Duke. 2014. Assessment of vegetation and soil conditions in restored mangroves interrupted by severe tropical typhoon 'Chan-hom' in the Philippines. *Hydrobiologia* 733 (1): 85–102.

Sherman, Ruth E., Timothy J. Fahey, and Pedro Martinez. 2001. Hurricane impacts on a mangrove forest in the Dominican Republic: damage patterns and early recovery. *Biotropica* 33 (3): 393–408.

Smith, Thomas J., Michael B. Robblee, Harold R. Wanless, and Thomas W. Doyle. 1994. Mangroves, hurricanes and lightning strikes. *BioScience* 44 (4): 256–262. https://doi.org/10.2307/1312230.

Smith, Thomas J., Gordon H. Anderson, Karen Balentine, Ginger Tiling, Greg A. Ward, and Kevin R.T. Whelan. 2009. Cumulative impacts of hurricanes on Florida mangrove ecosystems: sediment deposition, storm surges and vegetation. *Wetlands* 29 (1): 24–34. https://doi.org/10.1672/08-40.1.

Smoak, J.M., J.L. Breithaupt, T.J. Smith III, and C.J. Sanders. 2013. Sediment accretion and organic carbon burial relative to sea-level rise and storm events in two mangrove forests in Everglades National Park. *Catena* 104: 58–66. https://doi.org/10.1016/j.catena.2012.10.009.

Spackman, W., C.P. Dolsen, and W. Riegel. 1966. Phytogenic organic sediments and sedimentary environments in the Everglades-mangrove complex. *Palaeontographica* 117: 135–152.

Troxler, T.G., E. Gaiser, J. Barr, J.D. Fuentes, R. Jaffe, D.L. Childers, L. Collado-Vides, et al. 2013. Integrated carbon budget models for the Everglades terrestrial-coastal-oceanic gradient: current status and needs for inter-site comparisons. *Oceanography* 26 (3): 98–107.

USEPA. 1993. *Methods for the determination of inorganic substances in environmental samples, EPA/600/R-93/100*. Washington: U.S. Environmental Protection Agency.

Vance, E.D., P.C. Brookes, and D.S. Jenkinson. 1987. An extraction method for measuring soil microbial biomass C. *Soil Biology and Biochemistry* 19 (6): 703–707. https://doi.org/10.1016/0038-0717(87)90052-6.

Whelan, Kevin R.T., Thomas J. Smith, Gordon H. Anderson, and Michelle L. Ouellette. 2009. Hurricane Wilma's impact on overall soil elevation and zones within the soil profile in a mangrove Forest. *Wetlands* 29 (1): 16–23. https://doi.org/10.1672/08-125.1.

Zhang, Keqi, Huiqing Liu, Yuepeng Li, Hongzhou Xu, Jian Shen, Jamie Rhome, and Thomas J. Smith. 2012. The role of mangroves in attenuating storm surges. *Estuarine, Coastal and Shelf Science* 102–103. Elsevier Ltd: 11–23. https://doi.org/10.1016/j.ecss.2012.02.021.